Building Technologies & Urban Systems Division
Energy Technologies Area
Lawrence Berkeley National Laboratory

Benefits assessment of cool skin and ventilated cavity skin: Saving energy and mitigating heat and grid stress

Jiwon Park[1], Kwang Ho Lee[1], Sang Hoon Lee[2], Tianzhen Hong[2]

[1]Department of Architecture, Korea University, Seoul, Republic of Korea,
[2]Building Technology and Urban Systems Division, Lawrence Berkeley National Laboratory, USA

Energy Technologies Area
January 2024

https://doi.org/10.1016/j.buildenv.2023.111027

This work was supported by the Assistant Secretary for Energy Efficiency and Renewable Energy, Building Technologies Office, of the US Department of Energy under Contract No. DE-AC02-05CH11231.

Disclaimer:

Building and Environment 247 (2024) 111027

Contents lists available at ScienceDirect

Building and Environment

journal homepage: www.elsevier.com/locate/buildenv

Benefits assessment of cool skin and ventilated cavity skin: Saving energy and mitigating heat and grid stress

Jiwon Park [a], Kwang Ho Lee [a], Sang Hoon Lee [b,*], Tianzhen Hong [b]

[a] Department of Architecture, Korea University, Seoul, Republic of Korea
[b] Building Technology and Urban Systems Division, Lawrence Berkeley National Laboratory, USA

ARTICLE INFO

Keywords:
Cool skin
Ventilated cavity skin
Future weather
Building energy
Thermal comfort
Thermal resilience

ABSTRACT

This study assessed the energy-saving and climate-adaptive potential of cool skin and ventilated cavity skin facade technologies in Seoul's high-rise apartment buildings. We created weather scenarios for historical, mid-term future, and long-term future conditions using Coordinated Regional Downscaling EXperiment (CORDEX) method. Building energy simulations were conducted on a South Korean high-rise apartment model to evaluate their performance under different weather conditions. The results indicate that cool skin and ventilated cavity skin technologies can save cooling energy during summers but lead to heating energy penalties in winters. Ventilated cavity skin outperforms cool skin, offering better cooling energy savings and reduced heating penalties. Combining both technologies yields the highest overall energy savings, with 7 %, 9 %, and 10 % cooling energy savings for cool skin, ventilated cavity skin, and the combined package, respectively. However, cool skin increases heating energy consumption by 5 %, while ventilated cavity skin has minimal impact on heating energy. These envelope technologies also reduce peak electricity demand by at least 5 %, 8 %, and 9 %, respectively. They contribute to heat stress reduction, enhance resilience, and decrease extreme heat risks for occupants during power outages by at least 18 % under various weather conditions. Considering the prevalence of aging high-rise apartments in South Korea, adopting these envelope renovation strategies can effectively reduce cooling loads, enhance thermal comfort, and boost resilience under future climates, while avoiding costly reconstruction.

1. Introduction

The growing global concern about climate change has sparked a movement towards achieving carbon neutrality [1]. In alignment with this shift, efforts are being made to reduce building energy consumption, which accounts for about one-third of global primary energy usage [2]. To address this challenge, a range of energy conservation measures and control strategies are being employed at the building level to diminish energy consumption and enhance operational efficiency.

Energy conservation measures in buildings can be broadly categorized into active solutions and passive solutions. Active measures encompass heating, ventilation, air conditioning (HVAC) systems, lighting, and other building service applications. Passive measures, such as envelope technologies, solar control windows, phase change materials, and shading technologies [3], incorporate energy-efficient architectural components to reduce energy consumption while enhancing indoor comfort [4].

With climate change progressing, the increasing occurrence of severe heatwaves is a major concern, posing substantial risks to human health [5]. During extreme events, extensive use of air conditioning can overload the power grid, resulting in frequent blackouts [6]. Therefore, it is essential to integrate passive measures to enhance building's resilience and ensure occupants' safety during power outages [7]. A study has shown that implementing passive design techniques can reduce peak cooling demand in buildings by up to 65 %, significantly lowering the power outage risk [8].

Envelope technologies, such as cool skin, effectively reduce building energy consumption [9]. Cool skin works by enhancing the solar reflectivity on a building's exterior, reducing the transfer of radiative heat into interior spaces [10]. Numerous have demonstrated that cool skin can lower cooling energy usage and stabilize building HVAC system [11,12]. However, it's crucial to consider the trade-off between cooling and heating energy when applying cool skin, depending on the local climate conditions. Research indicates that cool walls yield more

* Corresponding author. 1 Cyclotron Road Bldg 90-3111R, Berkeley, CA, 94720, USA.
E-mail address: sanghlee@lbl.gov (S.H. Lee).

https://doi.org/10.1016/j.buildenv.2023.111027
Received 21 August 2023; Received in revised form 31 October 2023; Accepted 10 November 2023
Available online 17 November 2023

significant annual energy savings in warmer climates [10].

Ventilated cavity skin, which is also known as Double skin façade (DSF), is an envelope strategy with the potential to conserve both heating and cooling energy. Ventilated cavity consists of a conventional facade, an air cavity, and an additional outer skin, typically made of glass [13]. But ventilated cavity skin also can be designed to have opaque outer skins. Sealed opaque ventilated cavity skin provide exceptional insulation, resulting in energy savings for heating in colder regions [14]. When the ventilated cavity skin is not connected to the indoor space, air circulates exclusively within the air cavity, effectively minimizing solar heat gain, therefore contributing to a reduction of inner surface temperatures. As a result, this DSF design approach minimizes cooling loads [15]. A study found that ventilated cavities can achieve a cooling demand reduction equivalent to that of 4 cm of insulation material in residential buildings [16]. However, this configuration may lead to heating energy penalties during the winter season [17]. In a study conducted in Japan's hot and humid climate, a 78 mm thick ventilated cavity roof was installed in a single-story large factory building. The results demonstrated that the roof could lower the inner surface temperature by approximately 4 °C compared to a conventional roof and reduce cooling load by approximately 50 % during the summer season [18].

The decision to implement these strategies is typically made during the building's design phase, where the energy performance of the structure is established in compliance with prevailing regulations and standards at the time of construction. However, the effects of climate change have introduced significant shifts in cooling and heating demands experienced by building occupants. This necessitates comprehensive research to evaluate the performance of existing buildings within this evolving environmental context. It is crucial to address the implications of transitioning toward higher cooling loads and lower heating loads due to global warming and develop effective strategies for mitigating the impact of extreme weather events [5]. In recognition of these challenges, the International Energy Agency (IEA) has launched Annex 80 – Resilient Cooling of Buildings, a collaborative initiative to evaluate the effectiveness of diverse building-resilient cooling strategies in ensuring the thermal comfort of occupants in the face of a changing climate [19].

East Asia, a highly vulnerable region significantly affected by climate change and extreme weather events [20], requires substantial investment in mitigation efforts, as indicated in the 2023 IPCC report [21]. Seoul, the capital city of South Korea, is a densely populated urban area where buildings collectively consume over 87 % of the city's electricity [22]. High-rise apartments are the most common type of housing in South Korea, accounting for more than 63 % of all residential buildings [23]. These high-rise apartment buildings have been constructed since 1962, a period of explosive economic growth, but energy design standards have evolved significantly over the past few decades [24,25]; the energy performance of older high-rise apartment buildings is poor and likely needs improvement compared to more recently constructed ones.

Reconstruction and renovation efforts are currently underway in Seoul to transform the dilapidated appearance of residential buildings into attractive ones [26]. However, for high-rise apartment buildings, huge-scale redevelopment and reconstruction are prioritized over renovation [27]. Recently, the increasing number of aging buildings and the issue of resource waste during this redevelopment process have raised the need for renovation technologies [28]. There is potential to apply facade technologies to improve the energy performance of the buildings in this process.

Recent commercial building renovations in South Korea have actively adopted ventilated cavity skin to enhance existing envelopes. However, the energy performance of this technology has yet to be thoroughly examined within the South Korean context. Since this approach affects only the opaque side of the building and does not impact the visual or lighting environment for occupants, it holds high potential for application in residential buildings.

This study assessed the energy-saving and resiliency effects of two widely employed facade technologies: cool skin, which is a highly versatile and resilient cooling envelope technology, and ventilated cavity skin, frequently used to enhance the visual appeal of building exteriors in Seoul, South Korea. The paper explores: (1) modeling and simulation of the cool skin and ventilated cavity skin facade technologies for high-rise apartments in Seoul, (2) development of the historical and future weather data for Seoul, and (3) evaluation of the energy and resilience performance and their benefits under the historical and future weather data. The outcomes can inform building designers in their decision to adopt the cool skin or ventilated cavity skin technologies during the renovation of high-rise apartment buildings in Seoul, considering the benefits in energy and thermal resilience under historical and future weather conditions.

2. Methodology

To evaluate the energy and thermal resilience performance of the cool skin and ventilated cavity skin technologies, we simulated their performance in the Korean context using historical and future weather data. Fig. 1 outlines the research workflow. We utilized EnergyPlus version 22.2, a widely recognized software for building energy simulations. During the simulation, we assumed that the building was situated in a city terrain. To calculate shadow effects from balconies, windows, and doors and determine solar radiation and reflectance, we employed the Full Exterior Solar Distribution method. The heat balance thermal analysis algorithm was used to calculate convection on interior surfaces by determining heat transfer coefficients based on temperature differences for various orientations. The DOE-2 algorithm was employed to calculate exterior surface convection using measurements for rough surfaces [29].

We used the South Korean high-rise apartment reference building energy model [30] developed by the South Korean Institute of Construction Technology (KICT) in 2017. In addition, we used weather data from the Seoul Observatory of the South Korean Meteorological Administration (KMA) (latitude 37.57, longitude 126.97, elevation 86 m), situated in ASHRAE climate zone 4A, representative of a mixed humid climate zone. To evaluate the building's performance under changing climate conditions, the historical and future weather data were developed based on the Coordinated Regional Downscaling EXperiment (CORDEX) method.

The CORDEX method is designed for regional-scale climate projections intended for impact assessment and adaptation studies. While coupled atmosphere-ocean general circulation models are commonly employed for predicting future weather conditions, they come with limitations due to their global scope and lower resolution in specific regions, making them less suitable for building energy simulations. To overcome this constraint, climate prediction researchers have developed methods to downscale these models to regional climate models with higher resolutions. In this research, we follow a previous study to reassemble CORDEX method results for generating climate condition files to be used in simulations [31]. In Section 3.1, we provide a detailed overview of the climate condition development process for its application in building energy simulations.

2.1. High-rise apartment reference building energy model in South Korea

The high-rise apartment is the most common residential building type in South Korea. The high-rise apartment reference building energy model was developed based on the 2014 Housing Survey conducted by the Ministry of Land, Infrastructure and Transport (MOLIT) [30]. The building consists of a total of 16 floors, with 8 units arranged on each floor, resulting in a total of 128 units. Fig. 2 shows the high-rise apartment reference building energy model screen captured from OpenStudio software [32].

It is assumed that each unit is occupied by a household of three

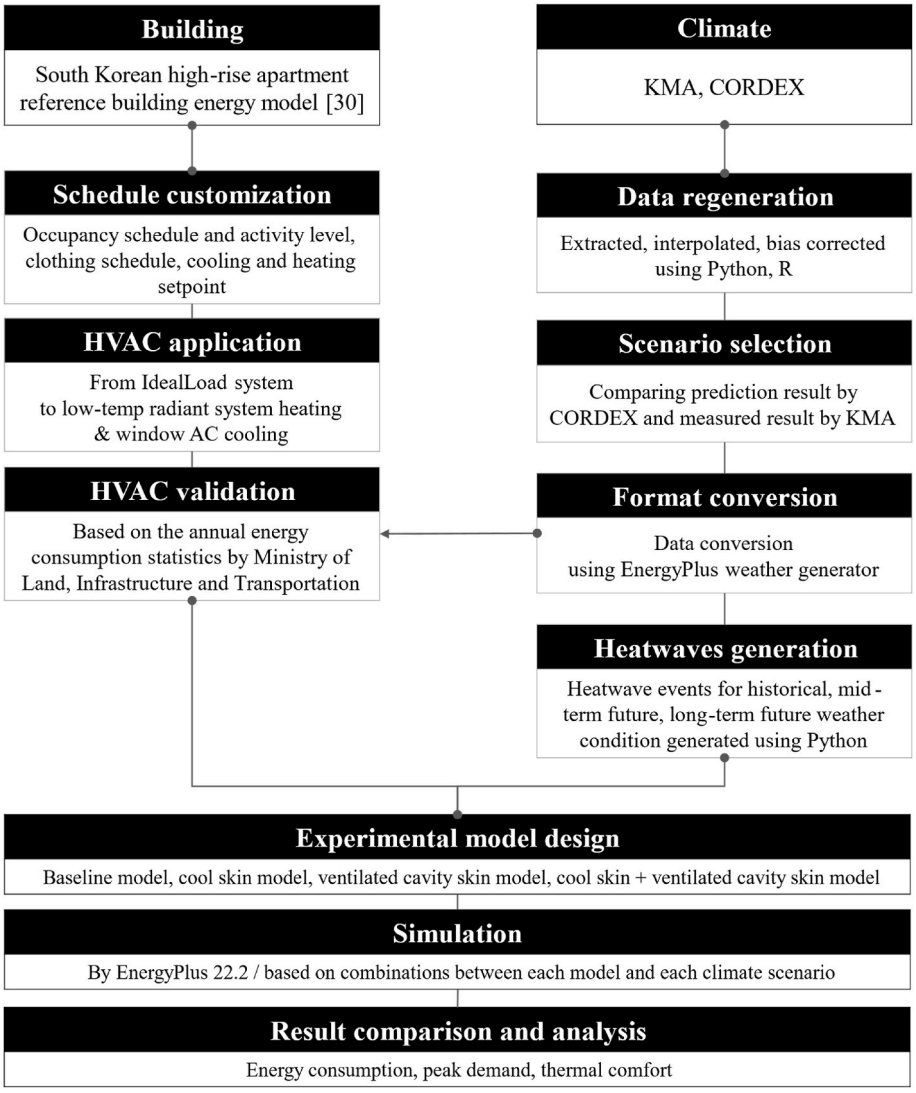

Fig. 1. Overall methodology flowchart of this research. The framework and interdependency paths between other processes are shown in the figure.

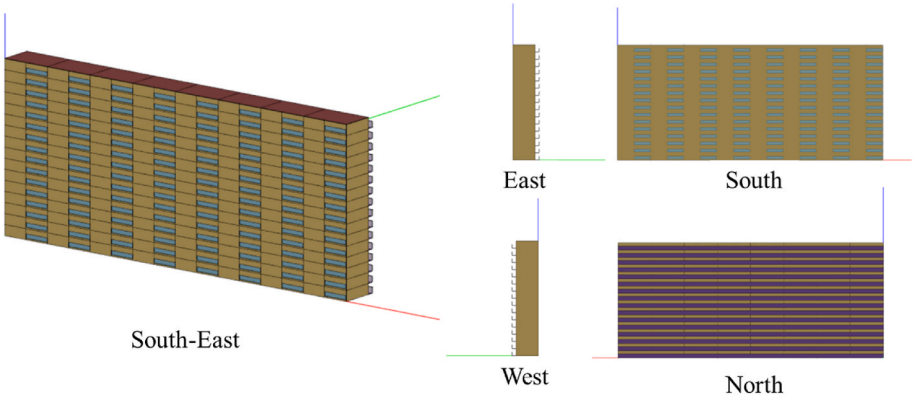

Fig. 2. South Korean high-rise apartment reference building model showing the 3D and elevation view by south, east, north, and west orientation using the OpenStudio software. The model has 16 floors and a total of 128 units.

people, and each unit is modeled as a single zone. Building energy performance standards and codes in South Korea were established in 1979 and have since undergone consistent revisions. Considering the thermal insulation performance of buildings is determined in accordance with these regulations, KICT developed four specific vintage year reference models which comply with significant revisions in building energy codes. Since this study focused on aging apartments requiring renovation, we used the 1980 construction condition model rather than the 1981–1988, 1989–2002, and 2003–2013 conditions. The building was set to maintain a summer cooling setpoint temperature of 24.9 °C

and a winter heating setpoint temperature of 21.0 °C. The schedules for electric devices, lighting fixtures, and other equipment were tailored to suit the local conditions in South Korea [30]. The characteristics of the high-rise apartment model for the study are as follows.

- Area per unit: 108 m^2
- Number of people per unit: 3
- Number of floors: 16
- Number of apartment unit: 128
- Construction vintage: 1980 construction condition
- Thermal transmittance (U-value): 1.07 W/m^2•K (wall), 1.05 W/m^2•K (roof), 1.10 W/m^2•K (floor), 5.00 W/m^2•K (window)
- Window solar heat gain coefficient: 0.83
- Window visible transmittance: 0.75
- Window to wall ratio: 18.7 % (total), 20 % (south, north), 0 % (east, west)
- Infiltration rate: 0.4 air changes per hour
- Light power density: 5.03 W/m^2•K
- Electric equipment power density: 1.55 W/m^2•K
- Natural gas equipment power density: 1.63 W/m^2•K
- Service hot water: 75 L/day/person

The original reference high-rise apartment energy model by KICT used the ideal loads of HVAC systems. To ensure research outcomes that better align with the South Korean context, the HVAC system was adjusted to reflect the most common system used in South Korea. The primary heating system is a low-temperature radiant system. The predominant cooling system is the window-type air conditioner. We updated the HVAC system of the reference high-rise apartment energy model to have each unit with a low-temperature radiant system and a window air conditioner. The low-temperature radiant system operates using hot water supplied from a district heating plant at a temperature of 60 °C. The window air conditioner is powered by the grid electricity. The HVAC system size was automatically determined using the Design Day data extracted from the TMY (Typical Meteorological Year) weather data and the algorithm integrated into EnergyPlus. For heating, the system considered the 99.6 % Heating Design Day, while for cooling, the 0.4 % Cooling Design Day was used. A sizing safety factor of 1.2 was applied for both heating and cooling. The HVAC system sizing was determined based on the baseline apartment building configurations, and this fixed sizing was used for the cool skin and ventilated cavity skin performance evaluation under various weather conditions. We validated the simulated baseline heating and cooling energy consumption against the measured data. We compared the energy use intensity (EUI) of the reference model and the statistical data provided by the South Korean Ministry of Land, Infrastructure, and Transportation (MOLIT).

2.2. Baseline model energy use intensity validation

Table 1 presents the simulated cooling and heating EUI of the baseline model and the measured average cooling and heating EUI of all residential buildings in South Korea. The measured data were provided by MOLIT [33,34]. It was observed that cooling energy consumption accounts for approximately 9 % of the heating energy consumption from the South Korean measured residential building energy data source, indicating the heating energy consumption is more dominant than the cooling energy consumption in residential buildings in South Korea. Note that the baseline model represents a high-rise apartment building constructed in 1980, while the MOLIT data encompasses all residential buildings constructed across all time periods. The cooling and heating EUI of the baseline building appears to be approximately 1.6 times higher than the average MOLIT cooling and heating EUI. It has been reported that apartments built between 1985 and 1987 in South Korea exhibit approximately 43 % higher heating EUI compared to those constructed between 2015 and 2017 [33]. South Korea's insulation codes underwent three revisions between 1980 and 1984. Considering these, we confirmed that our baseline model's cooling and heating EUI represents the residential apartment building for the pre-1980 condition.

Table 1
Cooling and heating energy use intensity (EUI) comparison between measured data by MOLIT for all residential buildings in South Korea and simulated data from the baseline high-rise apartment energy model.

Data source	Cooling EUI [kWh/m^2]	Heating EUI [kWh/m^2]	Cooling + heating EUI [kWh/m^2]	Cooling ratio [%]
Measured South Korean residential building average EUI by MOLIT	7.0	72.1	79.8	8.8
Simulated South Korean high-rise apartment reference building energy model EUI	11.4	121.0	132.4	8.6

2.3. Cool skin and ventilated cavity skin

The cool skin strategy involves the application of white paint, which has higher sunlight reflectivity compared to other colors, on the building's exterior walls. Cool skin offers cost-effective solutions for cooling energy saving benefits, and its popularity has been increasing steadily due to its simple application. However, a cool skin reduces heat gain from solar radiation by reflecting more sunlight, which can result in increased heating energy consumption during the winter season when solar heat is beneficial. Therefore, to assess the effectiveness of the cool skin technology comprehensively, it is crucial to compare the energy savings in cooling with the potential penalties in heating. In EnergyPlus, the cool skin was implemented by adding an additional white paint layer to the construction set of all exterior walls in south, east, north, and west orientations, as well as the roof. The characteristics of the added cool skin layer are as follows [35].

- Cool paint on walls: thickness 1 mm, thermal absorptance 0.9, solar absorptance 0.4
- Cool paint on roofs: thickness 1 mm, thermal absorptance 0.9, solar absorptance 0.2

In South Korea, the commercial building sector is actively pursuing various innovative facade renovation approaches. One approach aims to transform the appearance of old buildings by adding a narrow cavity on top of the existing structure and attaching a new facade layer. In the commercial sector, this enhances the aesthetic transformation of the facade by covering both the original walls and windows. When it comes to aging apartment buildings, reconstruction after demolition is more commonly chosen over renovation. However, recently there has been increased interest in renovation due to the significant costs and carbon emissions associated with the demolition and reconstruction process. In this regard, we investigated the benefits of utilizing the popular ventilated cavity skin, commonly used in the commercial sector, for renovation in aging apartment buildings. This investigation aims to promote active renovation in the residential building sector.

Ventilated cavity skin involves incorporating a thin cavity and an additional surface called a "baffle" between the original building surface and the external environment. Fig. 3 illustrates the positioning of the components of the ventilated cavity skin within the building envelope layout.

To conduct simulations to investigate the effects of a ventilated cavity skin, it is necessary to specify the material used for the baffle. Aluminum plates, known for their lightweight properties, have been used widely in the construction industry in South Korea. Considering that most Korean apartments have a white finish, it was assumed that a

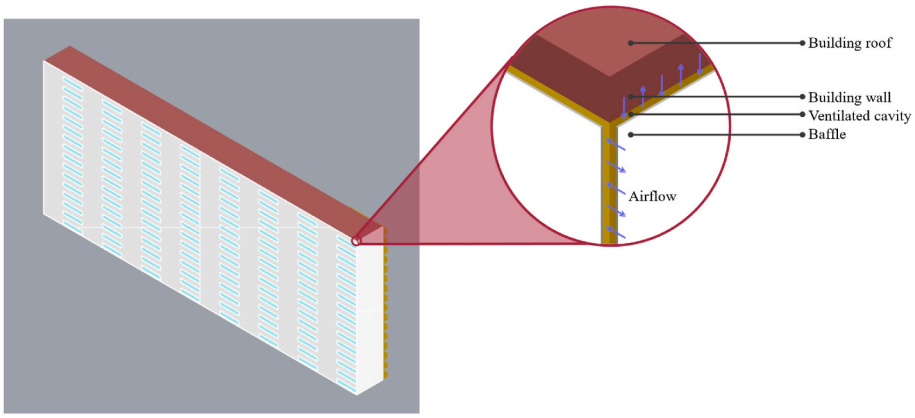

Fig. 3. Ventilated cavity skin components and layout when applied to the building envelope. The ventilated cavity skin includes an additional layer known as a baffle, as well as a ventilated cavity, installed over the general building wall.

whitewash finish would be preferred even after a retrofit. Therefore, we utilized whitewash on mirror-finished aluminum plates as baffles for modeling the ventilated cavity skin in EnergyPlus. The ventilated cavity skin was modeled using the "Exterior Natural Vented Cavity" object in EnergyPlus. This modeling approach ensures that all radiation reaching the surface of the baffle is reflected or absorbed and re-emitted as longwave radiation to the building surface.

To ensure the greatest annual energy savings from the optimal ventilated cavity skin design, a parametric study was conducted. The parametric study involved varying two key parameters of the ventilated cavity skin configuration: area fraction of openings and the thickness of the cavity. The "area fraction of openings" refers to an input parameter that quantifies the extent to which the amount of the baffle is open. It calculates the opening area by multiplying the building's surface area with the area fraction value. This study primarily aimed to assess the fundamental effects of ventilated cavity skin as a building envelope technology. To achieve this objective, we specifically selected the variant of ventilated cavity skin featuring a straightforward baffle design for evaluation. As a result, we used a 0.1 % of area fraction of opening near the ventilated cavity skin panel joints. The key ventilated cavity skin variables were as follows.

- Area fraction of openings: 0.1 %
- Thermal emissivity: 0.80
- Solar absorptivity: 0.19
- Thickness of cavity: 0.05 m

The installation of the ventilated cavity skin necessitates an additional structure for secure attachment of the baffle to the existing wall surface. Constructing the ventilated cavity skin is more intricate when dealing with non-flat wall surfaces. Additionally, the north facade presents spatial constraints due to balconies. Consequently, we implemented the ventilated cavity skin on the south, east, and west facades, as well as on the roof. The application of the ventilated cavity skin exclusively covered the building's opaque surfaces, ensuring that window areas remained intact to allow natural light into interior spaces, consistent with the baseline. Table 2 summarizes the total envelope area of the facades according to orientation and the portion covered by the ventilated cavity skin.

Table 2
Area of the ventilated cavity and overall exposed envelope per each elevation.

	Total [m^2]	South [m^2]	East [m^2]	North [m^2]	West [m^2]	Roof [m^2]
Envelope area	10,434	4417	366	4417	366	867
Ventilated cavity skin area	4665	3066	366	0	366	867

We examined the benefits of the individual cool skin and the ventilated cavity skin, and the integrated package of the cool skin and ventilated cavity skin. Table 3 summarizes the simulation cases of the envelope technologies.

3. Weather data development

This study developed historical and future weather data for use in EnergyPlus simulations to evaluate the energy performance and resilience of buildings with the cool skin, ventilated cavity skin, and package of cool skin and ventilated cavity skin under changing climate conditions. Three weather datasets were developed: the historical (2010s, 2000–2019), mid-term future (2050s, 2040–2059), and long-term future (2090s, 2080–2099) guided by Annex 80 [36]. These weather datasets were based on the RCP 8.5 scenario, which maintains the current carbon emissions in the future. This represents the most pessimistic scenario by the Intergovernmental Panel on Climate Change [37]. In building energy simulations, it is essential to have access to specific regional data. To address this need, the COordinated Regional Climate Downscaling EXperiment (CORDEX) provides future weather prediction data for 14 domains by downscaling the scope of global climate models [31].

The CORDEX data, future climate data generated by various research institutions, are available through the Earth System Grid Federation (ESGF) [38]. Those institutions provided high-resolution downscaled data specific to each region, capturing its unique climate characteristics. South Korea corresponds to the East-Asia (EAS) domain, and three models from this domain were utilized: (1) the MPI-*M*-MPI-ESM-MR model developed by the Max Planck Institute for Meteorology, downscaled using ICTP-RegCM4-4 (referred to as MPI), (2) the Ncc-NorESM1-M model developed by the Norwegian Climate Centre,

Table 3
Description of simulation cases of the envelope technologies.

Case	Description
Baseline	South Korean high-rise apartment reference building energy model
Cool skin	Baseline + white paint layer to exterior envelope surfaces on the south, east, north, west, and roof
Ventilated cavity skin	Baseline + additional ventilated cavity layer to the exterior surfaces on the south, east, west, and roof
Package of the cool skin and ventilated cavity skin (Package)	Baseline + white paint layer to exterior envelope surfaces on the south, east, north, west, and roof + an additional ventilated cavity layer to the exterior surfaces on the south, east, west, and roof

downscaled using ICTP-RegCM4-4 (referred to as NCC), and (3) the MOHC-HadGEM2-ES model developed by the Met Office Hadley Centre, downscaled using GERICS-REMO2015 (referred to as MOHC) [39–41]. We employed climate variables of dry bulb temperature, relative humidity, atmospheric pressure, wind speed, and global solar radiation (surface downwelling shortwave radiation) at an hourly scale. We generated hourly weather data for Typical Meteorological Year (TMY) for the historical, mid-term future, and long-term future conditions.

3.1. Historical and future TMY weather

The overall process of creating climate data involved five key steps, as illustrated in Fig. 4, which follows the guideline provided by Machard et al. (2020) [31]. First, data collection and extraction were performed to acquire the necessary data. While CORDEX provides the downscaled data, it still covers the entire East Asia region and consists of 3-h time steps. In this step, Python was utilized to extract and interpolate data specific to Seoul (latitude 37.57, longitude 126.97) to obtain hourly data suitable for building energy simulations. However, a bias was observed when comparing the extracted data with the actual observations in Seoul.

In Fig. 4(a), the temperature distribution over 20 years from the downscaled East Asia CORDEX model is compared with the actual data recorded by the KMA in Fig. 4(b). Differences in probability distribution between the CORDEX and actual data are evident. To address the observed bias, we employed the Multivariate Bias Correction algorithm (MBCn). This R-programmed algorithm allowed a comparison of observed and predicted variable distributions at the same time step. We used 2000s observed data from the KMA and predictions from three CORDEX models. By aligning the probability distributions, we adjusted the CORDEX predictions for the 2010s, 2050s, and 2090s based on the 2000s bias trends. Additionally, in line with a previous study [42], we corrected solar radiation after sunset to zero based on solar altitude.

In the third step of the process, a TMY was generated by utilizing the hourly data collected over a 20-year period. The modified data for the historical, mid-term future, and long-term future conditions, spanning 20 years with a 1-h time step, were further transformed into TMY datasets comprising a total of 8760 h. Additionally, heatwave scenarios were extracted from each 20-year dataset representing the historical, mid-term future, and long-term future conditions.

Fourth, we selected the most suitable CORDEX model for Seoul. Historical TMY data from the MPI, NCC, and MOHC models were compared with observed data from KMA to assess data distribution. A Pearson correlation analysis evaluated the correlation between the

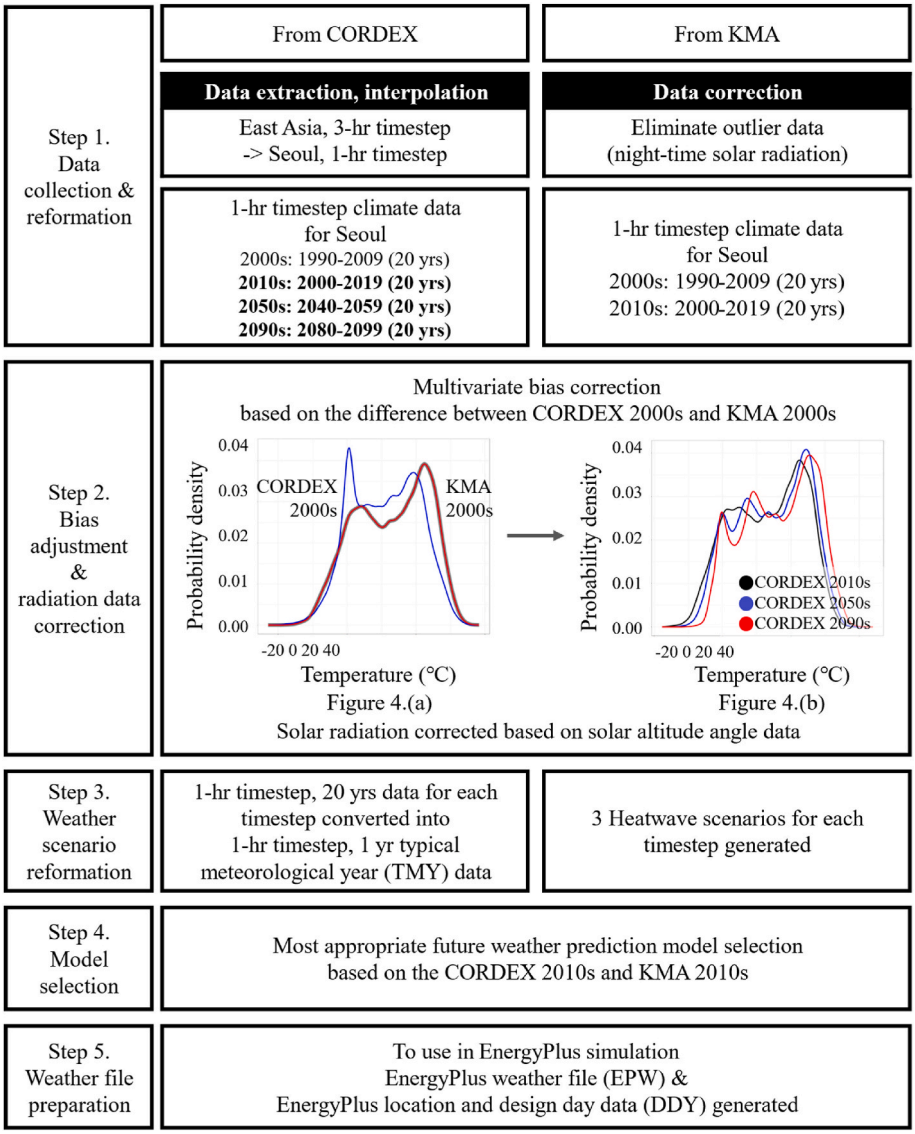

Fig. 4. Overall workflow to develop the historical and future weather data. Weather data development involves five key steps.

observed KMA data and the CORDEX results. The MPI model closely matched the observed data in terms of the annual distribution of temperature, solar radiation, and wind speed. It also did not exhibit the lowest correlation. Therefore, we chose the MPI model for climate scenarios.

Finally, we converted the developed weather data into EnergyPlus Weather Files (EPW) and EnergyPlus Location and Design Day data (DDY) files, formatted for EnergyPlus simulations.

Table 4 provides the characteristics of the developed historical and future weather data. It is evident that the average temperature exhibited a gradual increase from the historical condition to the mid-term and long-term future condition. Furthermore, the rate of change was expected to be higher from the mid-term to the long-term future condition compared to the change observed from the historical to the mid-term future. Alongside the rising average temperature, there is a corresponding increase in the cooling degree days (CDD) based on a threshold of 18 °C, indicating a greater need for cooling. Conversely, the heating degree days (HDD) based on a threshold of 10 °C exhibit a decrease, suggesting reduced heating requirements.

3.2. Heatwave weather scenarios

We established the heatwave threshold temperature by utilizing the 99.5th quantile of the 20-year temperature distribution, ensuring its adaptability across various geographical locations. Heatwave events occurred when temperatures exceeded this threshold. The duration and intensity of heatwaves were determined using the 97.5th quantile, based on the maximum daily mean temperature during this period. Heatwave severity was quantified as the cumulative temperature exceeding the 97.5th quantile threshold during the heatwave period. The end of a heatwave was defined when the temperature dropped to the 95th quantile [31].

Fig. 5 displays heatwave events in Seoul, South Korea, under various historical and future weather conditions. The circles' diameter represents the severity of each heatwave, while the x-coordinate indicates its duration, and the y-coordinate shows the maximum daily mean temperature. The color scheme distinguishes between historical (light yellow), mid-term future (yellow), and long-term future (dark yellow) heatwaves. Examining the progression from historical to long-term future conditions reveals increasing heatwave duration, intensity, and severity.

The most intense, severe, and prolonged heatwaves were extracted for each period, and the corresponding results are presented in Table 5. The heatwave with the highest maximum daily temperature is categorized as the most intense, while the heatwave with the largest severity value is considered the most severe. A clear pattern emerges when comparing the heatwave characteristics from the historical condition to the long-term future condition: there is a notable increase in the intensity, severity, and duration of heatwaves. It is particularly noteworthy that the heatwave duration reaches its peak in the long-term future condition, lasting for 53 days. These escalating trends in heatwave severity, intensity, and duration under projected future climatic conditions emphasize the need for heightened attention to building resilience.

4. Results and analysis

4.1. Annual cooling and heating primary energy use intensity savings

The high-rise apartment reference building energy model employs district heating for heating and electricity for cooling, which presents a challenge in comparing the effectiveness of energy conservation measures on heating and cooling energy consumption. To overcome this challenge, we followed the guidelines prescribed in the building energy efficiency rating certification system in South Korea [43], which utilizes primary energy as the standard for comparison. Primary energy consumption is calculated by multiplying the heating energy and cooling energy usage at the building site by the respective regional primary energy factors assigned to each energy carrier [44]. For this study, a site energy conversion factor of 2.75 was used for electricity, and a factor of 0.73 was used for district heating in South Korean buildings [43].

The baseline exhibited an increasing trend in cooling primary EUI and a decreasing trend in heating primary EUI over time. Fig. 6 illustrates the amount of saving in cooling primary EUI, and Fig. 7 illustrates the penalty in heating primary EUI for each weather condition. Under the historical weather condition, the cool skin demonstrated an approximate 9 % reduction in cooling primary EUI compared to the baseline. However, it also incurred a heating primary EUI penalty of about 4 %. When considering the overall impact on primary EUI, the cool skin resulted in an increase in total primary EUI under the historical weather condition, because heating consumes much more energy than cooling.

The ventilated cavity skin achieved approximately 11 % primary EUI savings in cooling compared to the baseline, with a minimal penalty on heating primary EUI under the historical weather condition. Thus, under the same weather and building conditions, the ventilated cavity skin exhibited a higher amount of reduction in cooling primary EUI and a lower heating primary EUI penalty compared to the cool skin. Moreover, the combined effect of cooling energy savings and heating energy penalties led to an annual reduction of primary energy consumption by over 3 kW-hours per square meter (kWh/m^2).

The package consisting of both the cool skin and ventilated cavity skin demonstrated greater cooling primary EUI savings: about 13 % in the historical weather condition. The heating primary EUI penalty remained negligible, resulting in an overall annual reduction in primary EUI of approximately 4 kWh/m^2. As the time passes from the historical weather condition to the short-term and long-term future conditions, the cooling demands increase. Consequently, the absolute amount of annual primary EUI savings exhibit a gradual increase and the percentage of annual primary EUI savings exhibit a gradual decrease for the cool skin, ventilated cavity skin, and package of cool skin and ventilated cavity skin.

4.2. HVAC peak electricity power reduction

To mitigate the risk of power outages during heatwave incidents, it is crucial to minimize the peak load on the energy grid. As previously mentioned, buildings in Seoul account for approximately 87 % of the city's electricity consumption [22]. Therefore, reducing the peak load from buildings is expected to reduce the occurrence of power outages significantly. This study analyzed the effects of cool skin and ventilated cavity skin technologies in reducing the peak HVAC electricity power

Table 4
Characteristic of the historical, mid-term future, and long-term future weather conditions of the MPI CORDEX model.

Year Coverage		Annual Average Temperature [°C]	CDD 18 °C	HDD 10 °C	Average Hourly Global Horizontal Solar Radiation During Sunshine [W/m^2]		
					Annual (Jan–Dec)	Summer (Jun–Aug)	Winter (Dec–Feb)
Historical (2010s)	2000–2019	13.3	780	1062	268	276	210
Mid-term future (2050s)	2040–2059	14.5	957	881	270	273	199
Long-term future (2090s)	2080–2099	16.2	1268	684	269	262	206

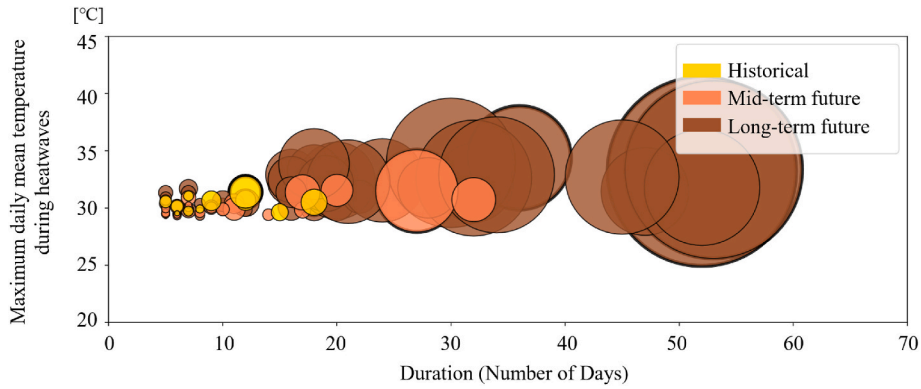

Fig. 5. Duration, maximum daily mean temperature, and severity trend of the historical, mid-term future, and long-term future condition heatwave events. The diameter of the circles indicates the severity of the heatwaves.

Table 5
Characteristics of heatwave scenarios of the historical, mid-term future, and long-term future weather conditions.

Year coverage	Heatwave type	Maximum daily mean temperature [°C]	Severity [°C ·hours]	Duration [days]	Heatwave start date (M/DD/YYYY)	Heatwave end date (M/DD/YYYY)
Historical	Most intense	31.4	13.9	12	7/30/2019	8/10/2019
	Most severe	31.4	13.9	12	7/30/2019	8/10/2019
	Longest	30.5	11.5	18	8/11/2006	8/28/2006
Mid-term future	Most intense	31.5	14.0	20	7/13/2057	8/01/2057
	Most severe	31.5	36.0	27	8/08/2054	9/03/2054
	Longest	30.7	19.2	32	7/29/2055	8/29/2055
Long-term future	Most intense	34.4	45.1	36	7/08/2086	8/12/2086
	Most severe	33.2	82.5	52	7/16/2083	9/05/2083
	Longest	33.4	77.5	53	6/30/2091	8/21/2091

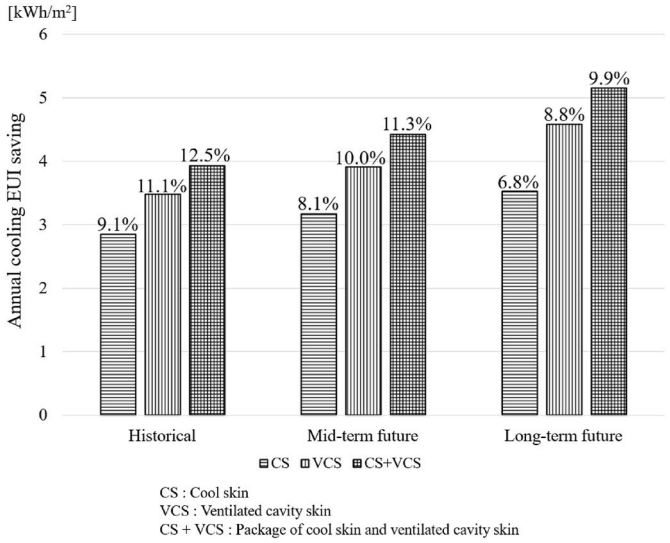

Fig. 6. Annual primary cooling energy use intensity saving. The figure presents both the absolute annual cooling energy use intensity (EUI) savings and the corresponding percentage of savings compared to the baseline.

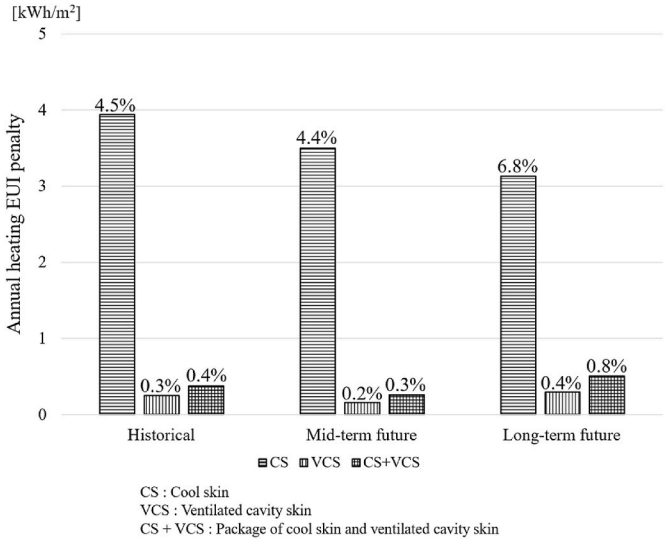

Fig. 7. Annual heating primary energy use intensity penalty. The figure presents both the absolute annual heating energy use intensity (EUI) penalties and the corresponding percentage of penalties compared to the baseline.

intensity (EPI) for a high-rise apartment reference building energy model. Fig. 8 illustrates the reduction in peak HVAC EPI for each model under different weather conditions. As time progresses from the historical to the mid-term and long-term future conditions, the peak HVAC EPI increases. The baseline exhibited a peak HVAC EPI of approximately 10.6 W per square meter (W/m^2) in the historical condition, 12.5 W/m^2 in the mid-term future condition, and 13.3 W/m^2 in the long-term future condition. Implementing the package of cool skin and ventilated cavity skin resulted in a 6 % and 9 % reduction in the peak HVAC EPI in the historical and mid-term future conditions, respectively. In the long-term future condition, the cool skin and ventilated cavity skin achieved reductions of 5 % and 8 % in the peak HVAC EPI, respectively. The package of cool skin and ventilated cavity skin exhibited outstanding effectiveness in reducing the peak HVAC EPI, with reductions of 9.7 %, 10.1 %, and 8.6 % in the historical, mid-term future, and long-term future conditions, respectively. Therefore, it is highly recommended to apply ventilated cavity skin, or a package of both cool skin and

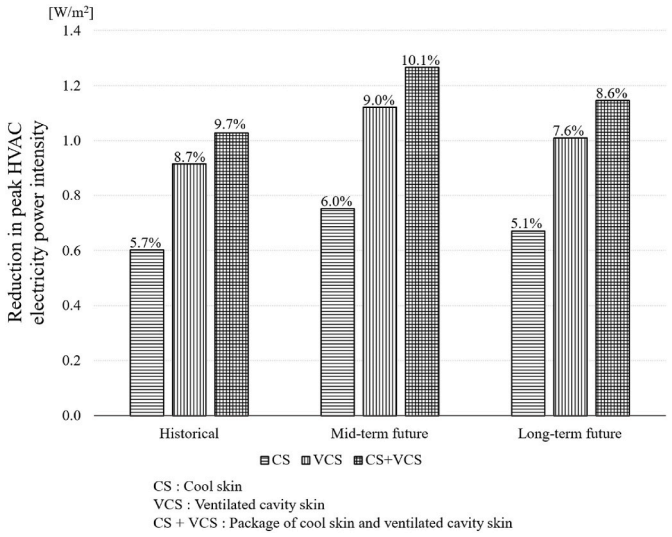

Fig. 8. Reduction in annual peak HVAC electricity power intensity for the historical, mid-term future, and long-term future conditions. The figure presents both the absolute reduction in peak heating, ventilating, and air conditioning (HVAC) electricity power intensity and the corresponding percentage of savings compared to the baseline.

ventilated cavity skin technologies to alleviate the strain on the power grid caused by climate change. These innovative building envelope technologies offer effective measures for reducing building energy consumption and mitigating the overall peak power intensity on the grid.

4.3. PMV-based thermal comfort improvement

We assessed the impact of cool skin, ventilated cavity skin, and the combination of both on occupants' thermal comfort using standardized methods from ISO 17772–1:2017, employing the Predicted Mean Vote (PMV) model for buildings with mechanical cooling and heating systems [45]. PMV predicts thermal sensation on a scale from −3 (cold) to +3 (hot) [46].

We analyzed annual PMV for a typical indoor apartment environment, considering an air velocity of 0.1 m/s, clothing insulation of 0.5 during summer (from May 1 to September 30) and 1.0 for other months, and a metabolic rate of 1.2 met. PMV calculations were conducted using the pythermalcomfort Python package [47], following the guidelines of the ASHRAE 55–2020 standard [48].

As per ISO 17772–1:2017 Annex H.1 Category III, a PMV above +0.7 indicates warmth discomfort in summer, while a PMV below −0.7 indicates coolness discomfort in winter [45]. Fig. 9 displays cumulative discomfort hours for baseline apartment units under historical, mid-term future, and long-term future weather conditions. We analyzed the PMV for apartment units located on the ground floor, middle floor, and top floor, including the west unit, center unit, and east unit. On the upper floors, we observed increased discomfort hours, likely due to exposed ceilings and direct solar radiation, resulting in greater influence from external conditions. These units experienced higher annual cooling and heating loads, leading to fluctuations that challenge meeting desired loads in real-time.

For historical conditions, ground and middle-floor units had around 120 discomfort hours, while top-floor units experienced approximately 350 discomfort hours, suggesting HVAC systems met most load requirements. However, moving to long-term future conditions, we observed increased discomfort hours, indicating the designed HVAC system sizing may struggle to meet future demands.

Subsequently, the evaluation of thermal comfort focused specifically on the east unit located on the top floor, which was identified as the most

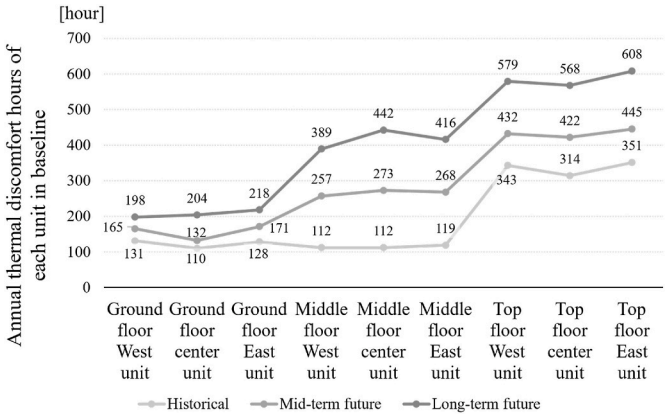

Fig. 9. Annual discomfort hours of each zone in the baseline for the historical, mid-term future, and long-term future conditions. It highlights the top floor East unit as the most vulnerable.

vulnerable unit based on the baseline across all weather conditions. Fig. 10 displays a boxplot illustrating the distribution of PMV values on an hourly basis throughout the year, considering the historical weather condition.

The baseline exhibits a negligible bias with a median PMV of 0.02, offering comfortable conditions for mechanically cooled and heated indoor spaces. Implementing cool skin, ventilated cavity skin, and a package result in median PMVs of −0.07, −0.04, and −0.04, respectively. These technologies maintain an acceptable PMV range without significant bias. Furthermore, the box length reduction indicates consistent comfort with cool skin, ventilated cavity skin, and the package approach.

This section focuses on the top-floor east unit to illustrate the effect of cool skin, ventilated skin, and the package on annual discomfort hours. *Warm discomfort hours*, with a PMV over 0.7, indicate a slightly warm perception, while *cool discomfort hours*, with a PMV below −0.7, imply a slightly cool perception. Fig. 11 displays the annual discomfort hours for the baseline, cool skin, ventilated cavity skin, and the package. Compared to the baseline, these strategies significantly reduced warm discomfort hours, with the combined approach showing the most substantial reduction. However, all models increased cold discomfort hours, although this penalty diminished over time from historical to long-term

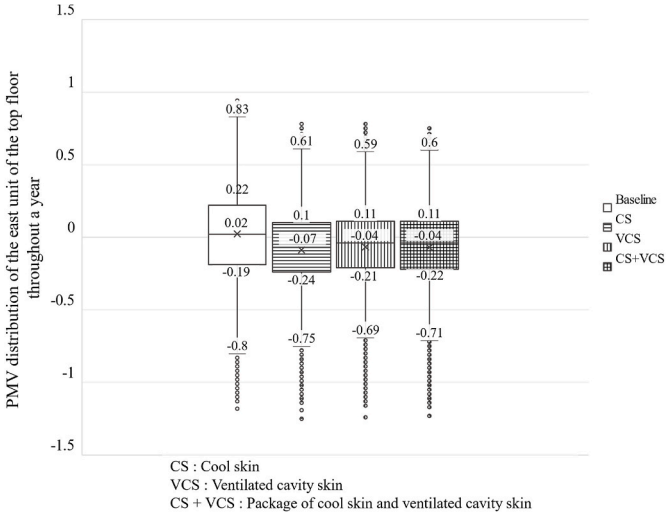

Fig. 10. Annual predicted mean vote (PMV) distribution of the east unit of the top floor in the baseline, cool skin, ventilated cavity skin, and package of cool skin and ventilated cavity skin for the historical condition. All the models exhibit a small bias.

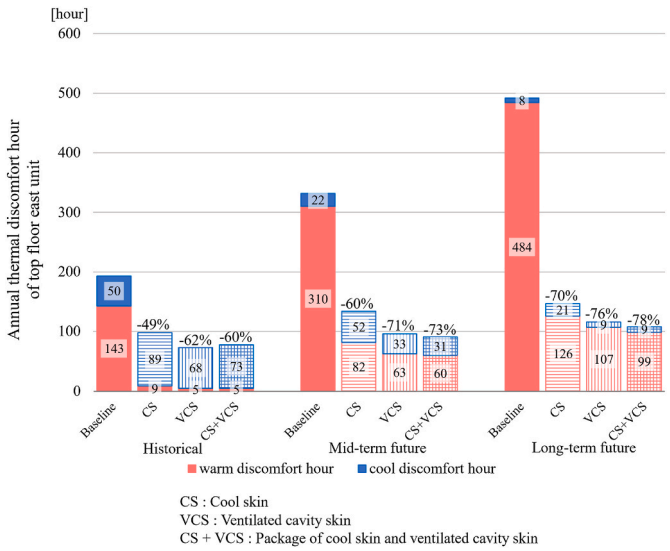

Fig. 11. Annual discomfort hours of the top floor east unit for the historical, mid-term future, and long-term future weather conditions. Cool skin, ventilated cavity skin, package of cool skin and ventilated cavity skin are effective in reducing the annual thermal discomfort hour of the most vulnerable unit, top floor east unit.

future conditions.

Cool skin minimally reduced warm discomfort hours by 49 %, while the ventilated cavity skin and package of cool skin and ventilated cavity skin achieved reductions of 62 % and 60 %, respectively. Under long-term weather conditions, the baseline's annual discomfort hours increased by approximately 500 h, but with the mentioned strategies, these values decreased by 70 %, 76 %, and 78 %, respectively.

4.4. Thermal comfort during heatwave scenarios

In addition to the annual thermal comfort analysis under the historical and future TMY conditions discussed in section 4.3, we evaluated the occupants' heat stress in extreme environmental conditions using heatwave weather year (HWY) data. We selected the most severe heatwave scenario from three weather conditions developed in Section 3.1. The most severe scenario represents the highest severity of heatwaves, where severity is evaluated based on the sum of the product of temperature exceedances above the threshold temperature at the 97.5 % quantile and their respective durations. Table 6 shows the heatwave climate characteristics for historical (2010s), mid-term future (2050s), and long-term future (2090s) periods.

This study adopted the Standard Effective Temperature (SET) methodology, as recommended by Annex 80, to assess human responses to heat stress [49]. SET represents the equivalent temperature of a virtual environment and occupant under specific conditions: 50 % relative humidity, 0.1 m/s air velocity, mean radiant temperature equal to the air temperature, 1.0 met activity level, and 0.6 clo clothing level for the occupant. The virtual environment ensures that the heat loss from an occupant's skin matches the heat loss in the actual environment [46]. Using the SET methodology, we comprehensively evaluated the impact of heat stress by comparing real thermal conditions with a virtual environment. This approach allowed for a detailed assessment of thermal strain during heatwaves, improving the accuracy of health risk assessments. A SET livable condition threshold of 30 °C was used to measure heat stress during heatwave events in free-running or mechanically cooled buildings with grid power outages [50].

Table 6
Characteristic of most severe heatwave events for the historical, mid-term future, and long-term future conditions.

	Maximum daily mean temperature [°C]	Severity [°C ·hours]	Duration [days]	Heatwave start date (M/DD/YYYY)	Heatwave end date (M/DD/YYYY)
Historical	31.4	13.9	12	7/30/2019	8/10/2019
Mid-term future	31.5	36.0	27	8/08/2054	9/03/2054
Long-term future	33.2	82.5	52	7/16/2083	9/05/2083

In this study, SET values were calculated using the pythermalcomfort Python package [47] based on the ASHRAE 55–2020 standard [48]. Fig. 12 presents SET values for various building models (baseline, cool skin, ventilated cavity skin, and the package) during a power outage period coinciding with the most severe heatwave event of the long-term future condition (from July 16 to September 5, 2083). This represents a worst-case scenario, considering that most power outages in Seoul's high-rise apartment buildings are typically resolved within 5 h [51]. Fig. 12 reveals that the baseline exceeds the 30 °C SET threshold for many hours, indicating occupants experience severe heat stress during the heatwave. However, all three technologies exhibit reduced SET values compared to the baseline, mitigating heat stress.

We calculated the SET degree-weighted hot exceedance hours (°C·hour), the sum of positive values of (difference between calculated SET and 30 °C) during occupied hours, to compare the heat stress among various heatwave events with the historical condition, mid-term future condition, and long-term future condition HWY data. Since heatwave durations vary by year (Table 6), the heatwave-total SET degree-weighted hot exceedance hours may not be the ideal metric. We normalized this metric to heatwave duration (°C ·hour/day) to compare outcomes from heatwaves of varying length. Fig. 13 presents the daily heat stress level represented with the daily SET degree-weighted hot exceedance hours.

Across all models, future heatwave events increased heat stress. The application of cool skin, ventilated cavity skin, and package of cool skin and ventilated cavity skin technologies contribute to reduce the heat stress by at least 20 %, 18 %, and 19 %, respectively. Through this heat stress reduction, even during extreme heatwave events in the long-term future conditions, the level of risks can be mitigated to a degree similar to the baseline in the historical condition.

In the historical condition, the package of cool skin and ventilated cavity skin demonstrated the most effective mitigation of SET exceedance weighted degree hours. However, in the mid-term future and long-term future conditions, the cool skin exhibited the best performance. The package of cool skin and ventilated cavity skin, with cool paint applied to the inner side of the baffle, showed minimal impact on reducing indoor temperatures, since the baffle already provides significant protection from solar radiation. The slight 1 % difference compared to the ventilated cavity skin was attributed to the cool skin installation on the north facade.

An analysis of the SET during heatwave periods revealed that envelope technologies played a role in mitigating SET distribution. However, despite this, it was found that a significant portion of time in all models exceeded the livable condition threshold. To examine the impact of the indoor environment on occupants' health during this period, the distribution of the Heat Index (HI) was investigated, and is discussed in this section. In this study, HI values were calculated using the pythermalcomfort Python package [47] based on the HI equation [52]. The U. S. Department of Commerce (DoC) uses the index of HI, which considers dry bulb temperature and relative humidity, to indicate the severity of indoor thermal environments [53]. It defines the range of 27–32 °C as corresponding to the *caution* category, where fatigue is possible with prolonged exposure and/or physical activity. The range of 32–41 °C falls under the *extreme caution* category, indicating that sunstroke, muscle cramps, and/or heat exhaustion are possible with prolonged exposure and/or physical activity. The range of 41–54 °C corresponds to the

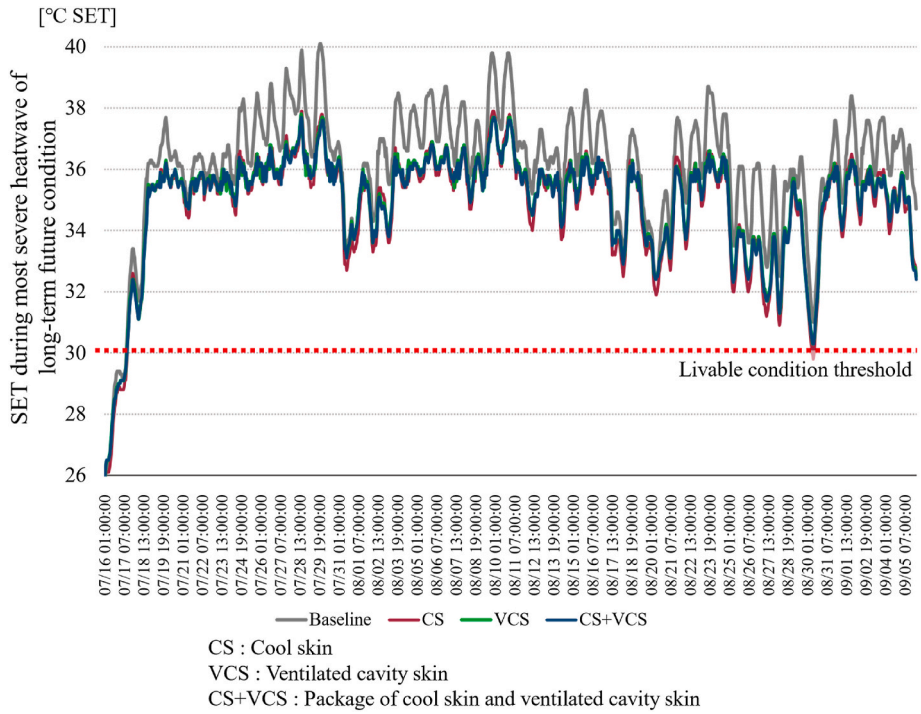

Fig. 12. Standard effective temperature (SET) trend during power outage caused by the most severe heatwave event of the long-term future condition (from July 16 to September 5 in 2083). All the models exhibit Standard Effective Temperatures above the livable condition threshold during the most severe heatwave in the long-term future condition.

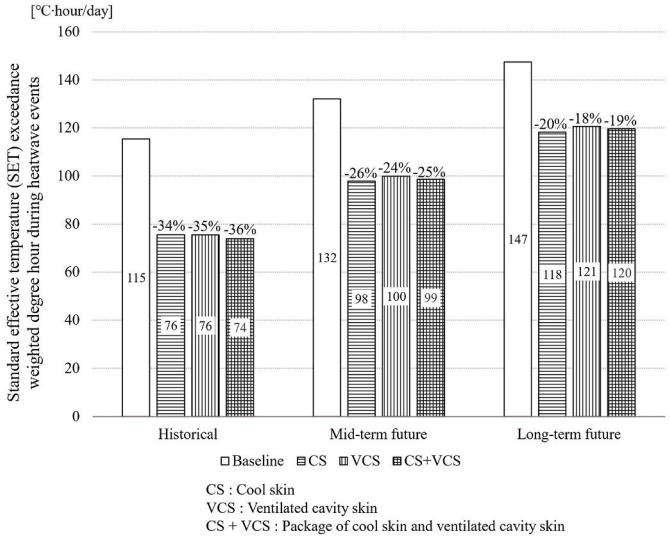

Fig. 13. The standard effective temperature (SET) exceedance weighted degree hours during the most severe heatwave events of the historical, mid-term future, and long-term future conditions. Cool skin, ventilated cavity skin, and the package of cool skin and ventilated cavity skin are effective in reducing standard effective temperature exceedance weighted degree hour during the most severe heatwave events.

danger category, where sunstroke, muscle cramps, and/or heat exhaustion are likely, and heatstroke is possible with prolonged exposure and/or physical activity. An HI above 54 °C indicates an *extreme danger* condition, where heatstroke or sunstroke is likely. Fig. 14 presents HI values for different models (baseline, cool skin, ventilated cavity skin, and package of cool skin and ventilated cavity skin) during a power outage period coinciding with the most severe heatwave event of the long-term future condition, from July 16 to September 5 in 2083. It was observed that cool skin, ventilated cavity skin, and the package of cool skin and ventilated cavity skin were all effective in alleviating HI during heatwave periods. In particular, they demonstrated the ability to prevent HI from exceeding the extreme danger threshold.

Fig. 15 illustrates cumulative hours at each HI hazard level during the most severe heatwave of long-term future condition. The baseline experienced 35 h of extreme danger, while the other three models did not reach the extreme danger category, indicating their excellent performance in reducing critical time periods. Although danger level hours were still present, a significant decrease in hours was observed. Therefore, it was confirmed that the cool skin, the package of cool skin and ventilated cavity skin, and the ventilated cavity skin were effective in reducing the severity of heatwaves.

5. Discussion

5.1. Envelope heat transfer analysis

We conducted a heat transfer analysis to assess the impact of cool skin and ventilated cavity skin technologies on energy consumption and thermal comfort. The analysis focused on radiative, convective, and conductive heat transfer between the interior and exterior surfaces of the south facade's center unit on the middle floor.

Radiative heat transfer on the exterior surface involves solar and longwave radiation between the wall's exterior and the surrounding environment [29]. The reference surface of the baseline experiences radiative heat transfer ranging from approximately 150 to 350 W/m^2 throughout the year, primarily indicating heat absorption by the building. Cool skin follows a similar pattern to the baseline throughout the year but with reduced radiative heat transfer. In contrast, both ventilated cavity skin and the package exhibit consistent radiative heat transfer with significantly lower values than the baseline and cool skin. This difference is attributed to the presence of a baffle in the ventilated cavity skin. The baffle reflects or absorbs solar radiation, reducing longwave radiation transmitted to the wall's exterior surface, leading to

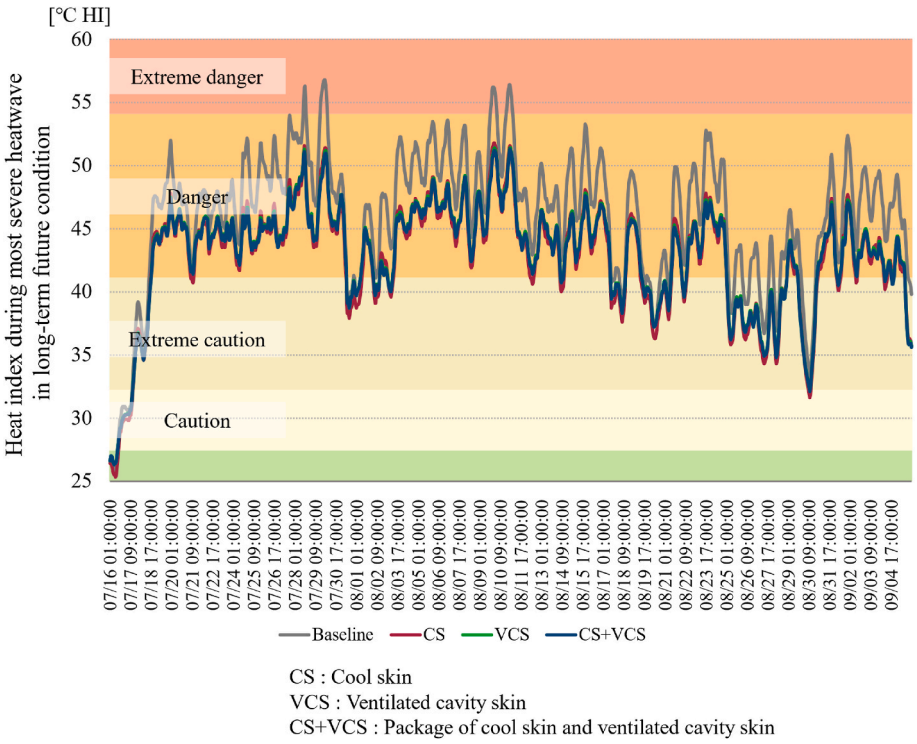

Fig. 14. Heat index during the most severe heatwave in the long-term future condition. Cool skin, ventilated cavity skin, the package of cool skin and ventilated cavity skin are effective in mitigating heat index during most severe heatwave in long-term future condition.

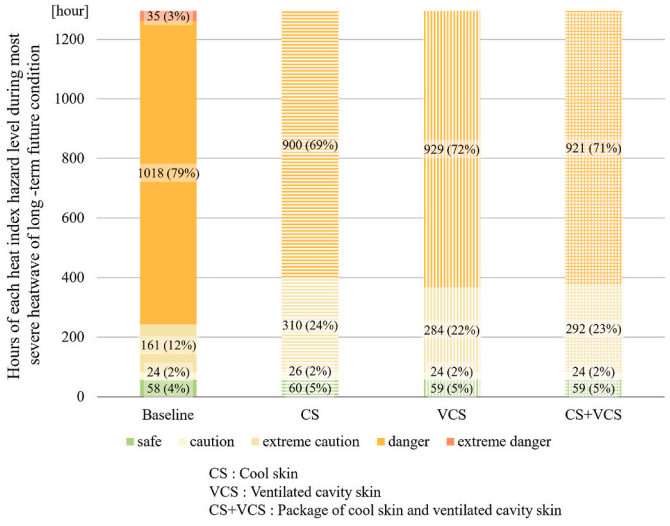

Fig. 15. Hours of each heat index (HI) hazard level and their percentage during the most severe heatwave of the long-term future for top floor east unit. Cool skin, ventilated cavity skin, the package of cool skin and ventilated cavity skin are effective in eliminating extreme danger heat index hazard level during most severe heatwave in long-term future condition.

significantly reduced radiative heat transfer.

Convective heat transfer encompasses forced and natural convection mechanisms. In the baseline, convective heat transfer primarily indicates negative values, representing heat dissipation from the building's interior. The analysis reveals that convective heat transfer through the reference surface during the winter season, characterized by a substantial indoor-outdoor temperature differential (approximately 270 W/m^2), is greater than in the summer season (approximately 100 W/m^2). Cool skin shows a similar annual trend of convective heat transfer as the baseline but with reduced magnitudes. Conversely, both the ventilated cavity skin and the package exhibit consistent convective heat transfer throughout the year with significantly reduced magnitudes. The baffle on the ventilated cavity skin reduces direct wind impact and radiative heat transfer, resulting in a notable decrease in forced and natural convection.

Conductive heat transfer of the reference surface from the exterior to the interior of the building wall is illustrated in Fig. 16. Cool skin exhibits a reduced but similar annual distribution of conductive heat

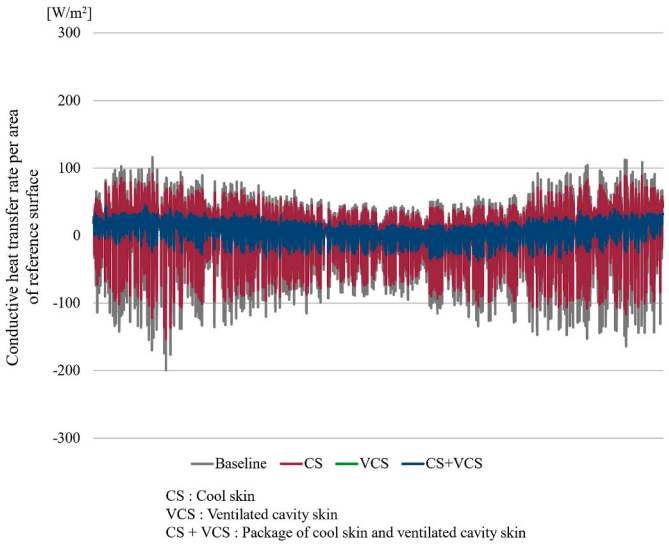

Fig. 16. Conductive heat transfer through the middle floor center unit for the baseline, cool skin, ventilated cavity skin, and package of cool skin and ventilated cavity skin of the historical weather condition. Ventilate cavity skin and the package of cool skin and ventilated cavity skin exhibit almost the same distribution.

transfer compared to the baseline, while ventilated cavity skin and the combination of cool skin and ventilated cavity skin maintain a consistent distribution throughout the year.

The significant reduction in annual radiative heat transfer achieved with cool skin leads to a substantial decrease in conductive heat transfer, resulting in a significant reduction in annual cooling energy consumption. In contrast, the ventilated cavity skin demonstrates diminished levels of radiative and convective heat transfer throughout the year, maintaining a relatively uniform distribution in conductive heat transfer. This characteristic results in a reduction in both cooling and heating energy consumption. The combination of cool skin and ventilated cavity skin behaves similarly to the ventilated cavity skin on the south facade, but the north facade acts as cool skin, resulting in more significant energy savings for cooling and increased heating energy penalties.

The radiative, convective, and conductive heat transfer analysis exhibits that implementing the ventilated cavity skin reduces the impact of external conditions, ensuring consistent heat transfer throughout the year, even in harsh climatic conditions. This maintains a mild operating environment for the building.

5.2. Selection of baffle material

To investigate the energy saving potential of ventilated cavity skin considering different baffle materials, additional materials were examined alongside the previously analyzed whitewash on a mirror-finished aluminum plate baffle. Table 7 presents the annual energy consumption results of various baffle materials. Although all components of the ventilated cavity skin had identical configurations, except for solar absorptivity and thermal emissivity, it was observed that these two variables resulted in diverse annual cooling and heating energy compositions.

In South Korea, where heating energy consumption accounts for 90 % of HVAC energy consumption, the ventilated cavity skin with an aluminum baffle exhibited the highest primary energy savings. It demonstrated notable reductions in both heating and cooling energy consumption. Conversely, the whitewash on a mirror-finished aluminum plate ventilated cavity skin used in this study showcased excellent cooling energy-saving effects, but the impact on heating energy savings was minimal, resulting in a comparatively lower overall primary energy saving.

A parametric study was undertaken to investigate the impact of thermal emissivity and solar absorptivity variations in the baffle on energy savings in the ventilated cavity skin. Fig. 17 illustrates the annual primary EUI trend. Blue indicates an increase in annual energy savings, while red represents a penalty. It was observed that higher thermal emissivity and lower solar absorptivity in the baffle contribute to enhanced cooling energy savings but result in greater heating energy penalties. Certain combinations of thermal emissivity and absorptivity yielded savings in both cooling and heating, while others incurred significant penalties. Therefore, thermal characteristics of baffle material needs to be carefully evaluated based on climate.

Table 7
Thermal characteristics and cooling and heating primary energy saving intensity of a baffle material for the historical condition [54].

Construction material	Solar absorptivity	Thermal emissivity	Cooling energy saving [%]	Heating energy saving [%]	Total primary energy saving [kWh]
Whitewash on a mirror finished aluminum plate	0.19	0.80	11	0	44,850
Aluminum (matt-silver)	0.28	0.07	3	11	155,249
Stainless steel (matt-silver, unpolished finished)	0.42	0.23	1	10	131,310

As the load on the baffle increases, additional structures become necessary. Therefore, lightweight materials are preferred for the baffles. In this study, we used aluminum baffles finished with white-wash. We assessed the visual discomfort of pedestrians in the outdoor environment due to the additional envelope installation and its impact on light pollution using an indicator called retinal irradiance [55,56]. Literature have shown that retinal irradiance equal to or higher than 0.14 can lead to after-images in pedestrians, while 12.55 or higher can result in permanent eye damage [56]. When we simulated light pollution at nine points along the building's south facade where pedestrians walk, the results showed that the flash hour, during which after-images occur, was similar to the baseline. However, the average retinal irradiance of visual discomfort at these points was about 5.6 % higher for the baseline (2.34) compared to the ventilated cavity skin (2.47). Therefore, the installation of ventilated cavity skin may subject pedestrians to slightly more reflected sunlight from the envelope. Hence, when selecting baffle materials, it is recommended to consider their impact on the surrounding light environment.

5.3. Limitations and future work

This study has certain limitations that need to be acknowledged. First, various assumptions were made for the simulations. Each apartment unit was simplified into a single thermal zone, and all units were assigned identical thermostat setpoints. Additionally, the activity level, clothing level, and schedules of occupants were significantly simplified. However, in reality, occupants have individualized setpoints and exhibit diverse behaviors throughout the day, even regulating their comfort by adjusting clothing levels. Consequently, the assumptions made in this study may not fully capture the complexities of real-world scenarios.

Moreover, in practice, occupant comfort can be augmented through natural ventilation facilitated by openings and increased air velocity by ceiling fans. However, these elements were not considered in this study. Furthermore, this study used a South Korean high-rise apartment reference building energy model, having units arranged in a linear corridor layout, representing the context of the 1980s. Although the geometry of this reference model was designed to be representative by previous researchers [30], real-world apartments have varying shapes due to differences in the number of floors, aspect ratios, and other geometry-related characteristics, which could result in different energy-saving effects.

Moreover, the ventilated cavity skin could have various designs in terms of material, color, shape, and the proportion of openings. However, this study focused on the most basic form of ventilated cavity skin. As analyzed in Section 5.3, the behavioral characteristics of the ventilated cavity skin could vary based on its design. Thus, it is advisable to compare the effects of various designs and select the optimal design after thorough evaluation.

Another consideration is that Seoul is a densely populated city, and the microclimate may vary significantly depending on surrounding buildings and the environment. However, in this study, we used measured weather data from the Seoul Observatory of the KMA. While the observatory is located in the central area of Seoul, it is surrounded by green areas, making it challenging to represent the microclimate of densely built-up regions.

Hence, future research directions are suggested as follows.

1. Conduct a study that minimizes uncertainties in simulation results.
2. Explore the benefits of strategies that consider natural ventilation and the use of ceiling fans.
3. Investigate the advantages of ventilated cavity skin in buildings with diverse geometries.

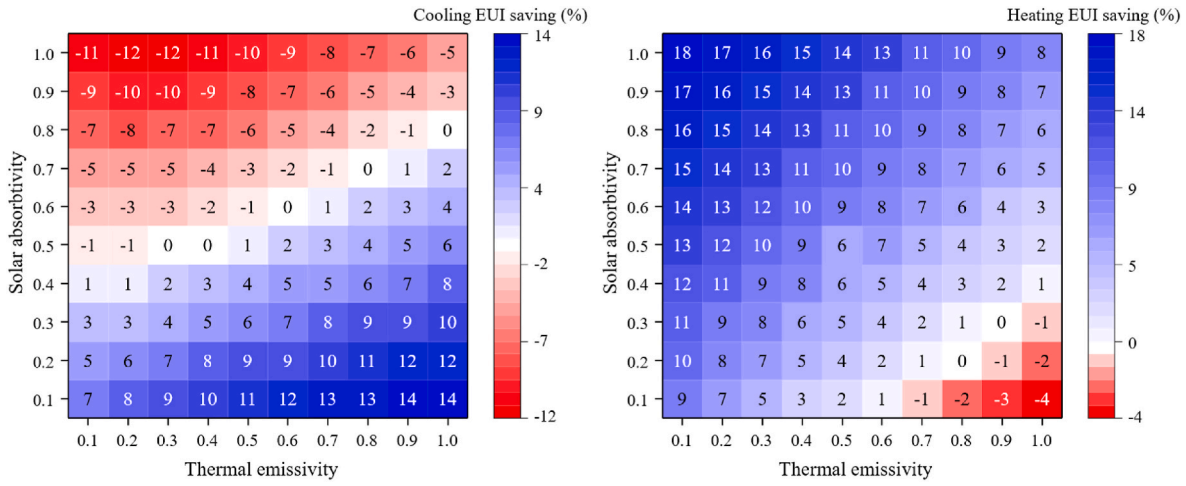

Fig. 17. Cooling and heating primary energy use intensity saving differences by the thermal characteristics of the baffle. Solar absorptivity and thermal emissivity affect annual cooling and heating energy use intensity savings and penalties.

4. Compare the advantages of various designs of ventilated cavity skin.
5. Conduct a study on the benefits of ventilated cavity skin that accounts for the microclimate of Seoul.

We can significantly advance understanding and practical implementation by addressing these limitations and pursuing future research directions. This progress will play a crucial role in future sustainable and energy-efficient building practices.

6. Conclusions

This study evaluated the energy performance, thermal comfort, and thermal resilience of envelope renovation methods using cool skin and ventilated cavity skin technologies, focusing on aged high-rise apartment residential buildings in Seoul, South Korea, under historical and future weather conditions. To evaluate the performance of the envelope technologies, building energy simulations were conducted using the EnergyPlus engine and a South Korean high-rise apartment reference building energy model. The energy simulations included the cool skin, ventilated cavity skin, and package of cool skin and ventilated cavity skin added to the high-rise apartment baseline building with 1980 construction conditions under historical (2010s), mid-term future (2050s), and long-term future (2090s) weather conditions. The weather data were developed based on the RCP 8.5 scenario using the CORDEX methodology.

For all the weather conditions, the cool skin and ventilated cavity offer cooling energy savings during the summer season but induce a heating energy penalty during the winter season. The ventilated cavity skin outperformed the cool skin, showing greater cooling energy savings and less of a heating energy penalty. The package of a cool skin and ventilated cavity skin showcased the greatest overall energy savings from the increased cooling energy savings. Cooling energy savings can be achieved by at least 7 %, 9 %, and 10 % from the cool skin, ventilated cavity skin, and package, respectively, for all weather conditions. However, the cool skin may lead to about a 5 % heating energy consumption increase. Therefore, it was confirmed that the cool skin strategy is well-suited for regions with high cooling EUI and either no or low heating EUI. The ventilated cavity skin can maintain the heating energy consumption at about the same level to the baseline. The peak electricity power demand by the building sector happens on a hot summer day, and these envelope technologies can offer by at least 5 %, 8 %, and 9 % peak electricity demand reduction from the cool skin, ventilated cavity skin, and package, respectively. When applying the ventilated cavity skin, baffle materials influence the performance in cooling and heating energy consumption. In regions with high cooling EUI, it is expected that using materials with high thermal emissivity and low solar absorptance will contribute to annual energy savings. Conversely, in areas with high heating EUI, using materials with low thermal emissivity and high solar absorptance is anticipated to be beneficial for annual energy conservation.

Upon examining the temporal progression from the historical to the long-term future conditions, it becomes evident that heatwaves are progressively increasing in duration, intensity, and severity. We used the most severe heatwave year weather data to evaluate the heat-related stress hours using the SET metric and heat-related danger hours using the heat index metric during the heatwave period. The cool skin, ventilated cavity skin, and the package contribute to mitigating heat-related health risks for apartment residents during heatwaves. In the case of a grid power interruption during heatwave events, heat stress of the most vulnerable unit can be reduced by at least 20 %, 18 %, and 19 % from applying the cool skin, ventilated cavity skin, and package, respectively. Also, all units do not face the extreme danger condition as measured by the heat index metric when any of these envelope technologies are added to a high-rise apartment building for all weather conditions. The future weather data show increased CDD and decreased HDD, which suggests that more attention must be given to the increased cooling load from buildings in the future. As high-rise apartments are the most common housing types of residential buildings in South Korea, and they are aging, envelope renovations using the cool skin, ventilated cavity skin and package strategies can play a key role in cooling load reduction, thermal comfort, and resilience improvement to address future climate change conditions while avoiding high reconstruction costs.

CRediT authorship contribution statement

Jiwon Park: Writing – original draft, Methodology, Data curation, Conceptualization. **Kwang Ho Lee:** Writing – review & editing, Supervision, Funding acquisition. **Sang Hoon Lee:** Writing – review & editing, Supervision, Methodology, Conceptualization. **Tianzhen Hong:** Writing – review & editing, Supervision.

Declaration of competing interest

All co-authors declare there is no conflict of interest in the reported work.

Data availability

Data will be made available on request.

Acknowledgments

This work was supported by the Korea Institute of Energy Technology Evaluation and Planning (KETEP) and the Ministry of Trade, Industry & Energy (MOTIE) of the Republic of Korea (No. 20224000000560), and National Research Foundation of Korea (NRF) grant funded by the Korea government (MSIT) (No. RS-2023-00217322).

References

[1] B.K. Sovacool, Expanding carbon removal to the global south: thematic concerns on systems, justice, and climate governance, Energy Clim. Change. 4 (2023), 100103, https://doi.org/10.1016/j.egycc.2023.100103.
[2] International Energy Agency, Buildings, IEA. (n.d.). https://www.iea.org/reports/buildings (accessed March 25, 2023).
[3] Y. Elaouzy, A. El Fadar, Energy, economic and environmental benefits of integrating passive design strategies into buildings: a review, Renew. Sustain. Energy Rev. 167 (2022), 112828, https://doi.org/10.1016/j.rser.2022.112828.
[4] X. Sun, Z. Gou, S.S.-Y. Lau, Cost-effectiveness of active and passive design strategies for existing building retrofits in tropical climate: case study of a zero energy building, J. Clean. Prod. 183 (2018) 35–45, https://doi.org/10.1016/j.jclepro.2018.02.137.
[5] C. Zhang, O.B. Kazanci, R. Levinson, P. Heiselberg, B.W. Olesen, G. Chiesa, B. Sodagar, Z. Ai, S. Selkowitz, M. Zinzi, A. Mahdavi, H. Teufl, M. Kolokotroni, A. Salvati, E. Bozonnet, F. Chtioui, P. Salagnac, R. Rahif, S. Attia, V. Lemort, E. Elnagar, H. Breesch, A. Sengupta, L.L. Wang, D. Qi, P. Stern, N. Yoon, D.-I. Bogatu, R.F. Rupp, T. Arghand, S. Javed, J. Akander, A. Hayati, M. Cehlin, S. Sayadi, S. Forghani, H. Zhang, E. Arens, G. Zhang, Resilient cooling strategies – a critical review and qualitative assessment, Energy Build. 251 (2021), 111312, https://doi.org/10.1016/j.enbuild.2021.111312.
[6] J.A. Casey, M. Fukurai, D. Hernández, S. Balsari, M.V. Kiang, Power outages and community health: a narrative review, Curr. Environ. Health Rep. 7 (2020) 371–383, https://doi.org/10.1007/s40572-020-00295-0.
[7] M. Sheng, M. Reiner, K. Sun, T. Hong, Assessing thermal resilience of an assisted living facility during heat waves and cold snaps with power outages, Build. Environ. 230 (2023), 110001, https://doi.org/10.1016/j.buildenv.2023.110001.
[8] S. Liu, Y.T. Kwok, K.K.-L. Lau, W. Ouyang, E. Ng, Effectiveness of passive design strategies in responding to future climate change for residential buildings in hot and humid Hong Kong, Energy Build. 228 (2020), 110469, https://doi.org/10.1016/j.enbuild.2020.110469.
[9] A. Bruck, S. Diaz Ruano, H. Auer, Values and implications of building envelope retrofitting for residential positive energy districts, Energy Build. 275 (2022), 112493, https://doi.org/10.1016/j.enbuild.2022.112493.
[10] P.J. Rosado, R. Levinson, Potential benefits of cool walls on residential and commercial buildings across California and the United States: conserving energy, saving money, and reducing emission of greenhouse gases and air pollutants, Energy Build. 199 (2019) 588–607, https://doi.org/10.1016/j.enbuild.2019.02.028.
[11] H. Gilbert, T. Jacobs, S. Jeong, M. Pomerantz, D. Millstein, D. Norsby, A. Repinsky, R. Levinson, Heat Island Mitigation Assessment and Policy Development for the Kansas City Region, 2019, https://doi.org/10.20357/B7JG61.
[12] A.L. Pisello, V.L. Castaldo, C. Piselli, C. Fabiani, F. Cotana, Thermal performance of coupled cool roof and cool façade: experimental monitoring and analytical optimization procedure, Energy Build. 157 (2017) 35–52, https://doi.org/10.1016/j.enbuild.2017.04.054.
[13] S. Barbosa, K. Ip, Perspectives of Double skin façades for naturally ventilated buildings: a review, Renew. Sustain. Energy Rev. 40 (2014) 1019–1029, https://doi.org/10.1016/j.rser.2014.07.192.
[14] N. Hashemi, R. Fayaz, M. Sarshar, Thermal behaviour of a ventilated Double skin facade in hot arid climate, Energy Build. 42 (2010) 1823–1832, https://doi.org/10.1016/j.enbuild.2010.05.019.
[15] A.L.S. Chan, T.T. Chow, K.F. Fong, Z. Lin, Investigation on energy performance of Double skin façade in Hong Kong, Energy Build. 41 (2009) 1135–1142, https://doi.org/10.1016/j.enbuild.2009.05.012.
[16] E. Bannier, V. Cantavella, M. Pinazo, M. Soto, G. Silva Moreno, Contribution of the ventilated façade to building energy demand, in: Castellón - Spain, 2019. https://www.researchgate.net/publication/336391073_Contribution_of_the_ventilated_facade_to_building_energy_demand. (Accessed 25 May 2023).
[17] C.-A. Domínguez-Torres, Á.L. León-Rodríguez, R. Suárez, A. Domínguez-Delgado, Empirical and numerical analysis of an opaque ventilated facade with windows openings under mediterranean climate conditions, Mathematics 10 (2022) 163, https://doi.org/10.3390/math10010163.
[18] L. Susanti, H. Homma, H. Matsumoto, A naturally ventilated cavity roof as potential benefits for improving thermal environment and cooling load of a factory building, Energy Build. 43 (2011) 211–218, https://doi.org/10.1016/j.enbuild.2010.09.009.
[19] P. Holzer, P. Cooper, IEA EBC Annex 80 on Resilient Cooling for Residential and Small Non-residential Buildings Annex Text, 2019.
[20] Q. You, Z. Jiang, X. Yue, W. Guo, Y. Liu, J. Cao, W. Li, F. Wu, Z. Cai, H. Zhu, T. Li, Z. Liu, J. He, D. Chen, N. Pepin, P. Zhai, Recent frontiers of climate changes in East Asia at global warming of 1.5°C and 2°C, Npj Clim. Atmospheric Sci. 5 (2022) 1–17, https://doi.org/10.1038/s41612-022-00303-0.
[21] AR6 Synthesis Report: Climate Change 2023, (n.d.). https://www.ipcc.ch/report/ar6/syr/(accessed October 28, 2023).
[22] Seoul Solution, New Renewable Energy: One Less Nuclear Power Plant, Seoul Solut., 2018. https://seoulsolution.kr/en/content/3363. (Accessed 25 May 2023).
[23] Statistics Korea, Population Census (2021), (n.d.). https://kosis.kr/statHtml/statHtml.do?orgId=101&tblId=DT_1JU1501&conn_path=I2 (accessed May 25, 2023).
[24] M. Evans, H. Chon, B. Shui, S.-E. Lee, Country Report on Building Energy Codes in Republic of Korea, Pacific Northwest National Laboratory, 2009.
[25] S. Ham, G. Lee, A Quantitative Analysis of the Apartment Unit Types in South Korea, vol. 34, 2010, pp. 47–55.
[26] K.-H. Sho, D.W. Jeong, K.-Y. Yang, Changes of building facades by commercial building remodelling - relation between emotional evaluation and preference assessment -, J. Reg. Assoc. Archit. Inst. Korea. 16 (2014) 225–232.
[27] J.-H. Hwang, S.-H. Yang, J.-H. Park, Y.-S. Kwon, A study on the characteristics of the current building deterioration and remodeling situation in Korean cities, J. Urban Des. Inst. Korea. 17 (2016) 65–82.
[28] H.-P. Jo, J.-H. Oh, S.-S. Kim, A study on the target parts for envelope remodeling prototype to improve thermal performance of old multi-family residential buildings, J. Korean Inst. Archit. Sustain. Environ. Build. Syst. 11 (2017) 52–57.
[29] U.S. Department, Of Energy, Engineering Reference, U.S. Department of Energy, 2022. https://energyplus.net/assets/nrel_custom/pdfs/pdfs_v22.2.0/EngineeringReference.pdf.
[30] D.W. Kim, Y.M. Kim, S.H. Lee, W.Y. Park, Y.J. Bok, S.K. Ha, S.E. Lee, Development of Reference Building Energy Models for South Korea, 2017, https://doi.org/10.26868/25222708.2017.789.
[31] A. Machard, C. Inard, J.-M. Alessandrini, C. Pelé, J. Ribéron, A methodology for assembling future weather files including heatwaves for building thermal simulations from the European coordinated regional downscaling experiment (EURO-CORDEX) climate data, Energies 13 (2020) 3424, https://doi.org/10.3390/en13133424.
[32] R. Guglielmetti, D. Macumber, N. Long, OpenStudio: an Open Source Integrated Analysis Platform; Preprint, National Renewable Energy Lab. (NREL), Golden, CO (United States), 2011. https://www.osti.gov/biblio/1032670. (Accessed 21 June 2023).
[33] Ministry of Land, Infrastructure and Transport, enhanced energy efficiency through green building policies, such as strengthening insulation standards, Minist. Land Infrastruct. Transp. (2019). http://molit.go.kr/USR/NEWS/m_71/dtl.jsp?lcmspage=72&id=95082347. (Accessed 6 February 2023).
[34] Ministry of Land, Infrastructure and Transport, Statistics on Energy Consumption of Buildings by Main Use, 2020. https://www.greentogether.go.kr/sta/sta010101.do. (Accessed 6 June 2023).
[35] R. Levinson, E. Arens, C. Curcija, H. Gilbert, C. Kohler, S.H. Lee, S. Selkowitz, N. Yoon, H. Zhang, Methodology to Assess Performance of Resilient Cooling Technologies, Lawrence Berkeley National Laboratory, 2023.
[36] Anaïs Machard, Agnese Salvati, Mamak P. Tootkaboni, Abhishek Gaur, Jiwei Zou, Liangzhu Wang, Fuad Baba, Hua Ge, Facundo Bre, Emmanuel Bozonnet, Vincenzo Corrado, Xuan Luo, Ronnen Levinson, Sang Hoon Lee, Tianzhen Hong, Marcello Salles Olinger, Roberto Lamberts, Delphine Ramon, Hoang Ngoc Dung Ngo, Abantika Sengupta, Hilde Breesch, Nicolas Heijmans, Jade Deltour, Xavier Kuborn, Sana Sayadi, Bin Qian, Chen Zhang, Ramin Rahif, Shady Attia, Philipp Stern, Peter Holzer, Afshin Afshari, Typical and extreme weather datasets for studying the resilience of buildings to climate change and heatwaves, Scientific Data (2023) [Paper #: SDATA-23-00603A Accepted].
[37] IPCC, Representative Concentration Pathways (RCPs), 2023, in: https://sedac.ciesin.columbia.edu/ddc/ar5_scenario_process/RCPs.html. (Accessed 2 February 2023).
[38] ESGF-LLNL - Home | ESGF-CoG, (n.d.). https://esgf-node.llnl.gov/projects/esgf-llnl/(accessed January 14, 2023).
[39] Max Planck Institute for Meteorology, Wcrp CMIP5: Max Planck Institute for Meteorology (MPI-M) MPI-ESM-MR model output collection, Cent. Environ. Data Anal. (2017). http://catalogue.ceda.ac.uk/uuid/83035a56b0e3498694aed0f319a83d7c. (Accessed 14 January 2023).
[40] Norwegian Climate Centre, Wcrp CMIP5: Norwegian Climate Centre (NCC) NorESM1-M model output collection, Cent. Environ. Data Anal. (2017). http://catalogue.ceda.ac.uk/uuid/753310df96fa4d9ca74dd33b19bdf330. (Accessed 14 January 2023).
[41] Met Office Hadley Centre, Wcrp CMIP5: met Office Hadley Centre (MOHC) HadGEM2-ES model output collection, Cent. Environ. Data Anal. (2012). http://catalogue.ceda.ac.uk/uuid/216becee8a6844ba8f8f98b9f075a635. (Accessed 14 January 2023).
[42] G. Pernigotto, A. Prada, D. Cóstola, A. Gasparella, J.L.M. Hensen, Multi-year and reference year weather data for building energy labelling in north Italy climates, Energy Build. 72 (2014) 62–72, https://doi.org/10.1016/j.enbuild.2013.12.012.
[43] Korea Institute of (2020.8.4.), Energy Efficiency and Conservation, Korea Institute of Energy Efficiency and Conservation, 2020, https://beec.energy.or.kr/BC/BC04/BC04_05_002.do?no=5. (Accessed 6 June 2023).
[44] Iso, ISO 52000-1:2017 Energy Performance of Buildings — Overarching EPB Assessment — Part 1: General Framework and Procedures, 2017. https://www.iso.org/standard/65601.html.
[45] Iso, ISO 17772-1:2017 Energy Performance of Buildings — Indoor Environmental Quality — Part 1: Indoor Environmental Input Parameters for the Design and Assessment of Energy Performance of Buildings, 2017. https://www.iso.org/standard/60498.html.

[46] ASHRAE, ANSI/ASHRAE Standard 55-2017 Thermal Environmental Conditions for Human Occupancy, 2017. https://www.ashrae.org/technical-resources/standards-and-guidelines/read-only-versions-of-ashrae-standards.
[47] F. Tartarini, S. Schiavon, Pythermalcomfort: a Python package for thermal comfort research, SoftwareX 12 (2020), 100578, https://doi.org/10.1016/j.softx.2020.100578.
[48] ASHRAE, ANSI/ASHRAE Standard 55-2020: Thermal Environmental Conditions for Human Occupancy, 2020. https://www.ashrae.org/technical-resources/standards-and-guidelines/read-only-versions-of-ashrae-standards.
[49] C. Zhang, O.B. Kazanci, S. Attia, R. Levinson, S.H. Lee, IEA EBC Annex 80 - Dynamic Simulation Guideline for the Performance Testing of Resilient Cooling Strategies: Version 2, 2023. https://vbn.aau.dk/en/publications/iea-ebc-annex-80-dynamic-simulation-guideline-for-the-performance-2.
[50] U.S. Green Building Council, Passive Survivability and Back-Up Power during Disruption (LEED V4 Pilot Credit IPpc100), 2021. https://www.usgbc.org/credits/passivesurvivability. (Accessed 25 May 2021).
[51] B. Kim, Apartment Power Outage Incidents Have Increased by Approximately Three Times Compared to Last Year… With 85% Occurring during the Summer Season This Year, Daehan Econ, 2018. https://m.dnews.co.kr/m_home/view.jsp?idxno=201810151304021610911. (Accessed 25 July 2023).
[52] L.P. Rothfusz, The Heat Index "Equation" (Or, More than You Ever Wanted to Know about Heat Index), NWS S. Reg, Forth Worth, TX, 1990. https://www.weather.gov/media/ffc/ta_htindx.PDF.
[53] N. US Department of Commerce, Heat Index Chart, (n.d.). https://www.weather.gov/ffc/hichart (accessed June 27, 2023).
[54] V.C. Sharma, A. Sharma, Solar properties of some building elements, Energy 14 (1989) 805–810, https://doi.org/10.1016/0360-5442(89)90034-0.
[55] R. Danks, J. Good, R. Sinclair, Assessing reflected sunlight from building facades: a literature review and proposed criteria, build, Environ. Times 103 (2016) 193–202, https://doi.org/10.1016/j.buildenv.2016.04.017.
[56] C.K. Ho, C.M. Ghanbari, R.B. Diver, Methodology to assess potential glint and glare hazards from concentrating solar power plants: analytical models and experimental validation, J. Sol. Energy Eng. 133 (2011), https://doi.org/10.1115/1.4004349.